

The Effects of Pendant vs. Fused Thiophene Attachment upon the Luminescence Lifetimes and Electrochemistry of Tris(2,2'-bipyridine)ruthenium(II) Complexes

Lasse J. Nurkkala,^[a] Robert O. Steen,^[a] Henrik K. J. Friberg,^[a] Johanna A. Häggström,^[a] Paul V. Bernhardt,^[b] Mark J. Riley,^[b] and Simon J. Dunne*^[a]

Keywords: Luminescence / N ligands / Ruthenium / Ligand design / Cyclic voltammetry

The electrochemical and photophysical properties for a range of tris(2,2'-bipyridine)ruthenium(II) complexes in which a thiophene substituent is attached to one of the bipyridine ligands by either a pendant or a fused mode have been determined. The fused mode of attachment eliminates torsional movement between the thiophene unit and the chelating bipyridine, thereby offering optimal overlap between the π -systems of the chelating unit and the attached thiophene unit. The electrochemical properties of these complexes were found to be similar; however, the luminescence lifetimes and intensities (in CH₃CN at room temperature) were found to

be correlated to the mode of attachment. The longest luminescence lifetime was observed for the complex [Ru(bpy)₂(4-(thiophen-2-yl)-2,2'-bipyridine)]²⁺ (3000 ns), as compared to the prototypic [Ru(bpy)₃]²⁺ (1745 ns). This complex also had the highest quantum yield (0.045). In the four isomeric complexes, where the thiophene ring was fused to the *b* or *c* face of the pyridine ring, the lifetimes fell in the interval 275–1510 ns, and the quantum yield ranged between 0.0047 and 0.014.

(© Wiley-VCH Verlag GmbH & Co. KGaA, 69451 Weinheim, Germany, 2008)

Introduction

While still in its infancy, molecular electronics is quickly expanding to be one of the hottest areas of chemical research. Part of the allure of this area is that no one approach dominates the field, and prototypic systems have been established from a wide range of chemical structures. The conductivity of organic molecules such as oligoacetylenes, oligophenylenes and oligothiophenes (as *molecular wires*, the simplest functional units of a *molecular circuit*) has been found to be dependant upon the length of the conjugation path, together with their ability to establish a fully planar completely delocalised π -system.^[1] Such oligomers are rigid and beyond a certain length, the handling properties of these oligomers become problematic due to their poor solubility. In this regard, oligothiophenes offer some advantages due to their fully planar structures, ease of synthesis and substitution, and their stability to oxidation.^[2] However, a molecular wire is not an active component in a molecular circuit, and thus it must be connected to an energy or electron source/sink to fulfill its role. We

have chosen to use the well-studied [Ru(bpy)₃]²⁺ as an electron source due to the efficiency and stability of its excited state.^[3] Upon photoexcitation, by a metal-to-ligand charge-transfer (MLCT) process, the complex undergoes red luminescence from the ³MLCT triplet state. The lifetime of this state can then be used to reflect the ability of the complex to act as an energy or electron source/sink.

The coupling between an energy/electron source and its conducting unit is of great importance.^[4] In our previous study^[5] we examined the isomeric effects within the covalent coupling of oligothiophene units and 2,2'-bipyridine chelating units upon the electrochemical and photophysical properties of their [Ru(bpy)₂L]²⁺ complexes. It was found that coupling of the oligothiophene in the 6-position of the 2,2'-bipyridine unit led to quenching of all long-lived red luminescence. This is due to the energy of the metal-centred d–d transition being lowered for 6-substituted bipyridines, leading to competitive radiationless relaxation and quenching of the luminescence. Coupling through the 4-position produced lifetimes longer than that of the prototype [Ru(bpy)₃]²⁺, but when this motif was used as the chelating unit in bridged dimetallic compounds, only weak electronic coupling was observed, perhaps due to lack of coplanarity between the bipyridine and the bridgehead, resulting from interannular interaction. This led us to investigate a new coupling mode where the first member of the oligothiophene was fused to one of the *b* or *c* faces of the chelating unit, thereby ensuring absolute planarity between these subunits. In this work we present a comparison of the electro-

[a] Department of Biology and Chemical Engineering, Mälardalen University, Gamla Tullgatan 2, 63105 Eskilstuna, Sweden
Fax: 46-16-153710
E-mail: simon.dunne@mdh.se

[b] Department of Chemistry, School of Molecular & Microbial Sciences, University of Queensland, Brisbane 4072, Qld, Australia

Supporting information for this article is available on the WWW under <http://www.eurjic.org> or from the author.

chemical and photophysical properties of the four [Ru(bpy)₂L]²⁺ complexes formed from this new class of connectors, with those of the [Ru(bpy)₃]²⁺, [Ru(bpy)₂L1]²⁺ and [Ru(bpy)₂L2]²⁺, where **L1** is 6-(thiophen-2-yl)-2,2'-bipyridine and **L2** is 4-(thiophen-2-yl)-2,2'-bipyridine in order to establish an optimal connecting mode for these components in molecular electronic applications.

Results and Discussion

Synthesis

The complexes **C1–C13** were prepared from their respective ligands **L1–L13** (see Figures 1 and 2) by treating the ligands with *cis*-[Ru(bpy)₂Cl₂] in ethylene glycol. Addition of ammonium hexafluorophosphate to the cooled reaction mixture resulted in precipitation of the complexes.

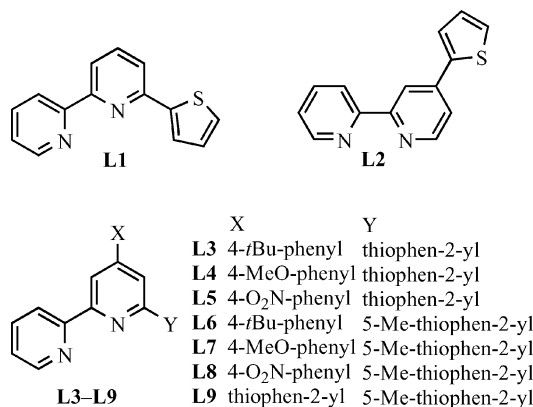


Figure 1. The thiophenyl-bipyridine ligands **L1–L9** used in this study.

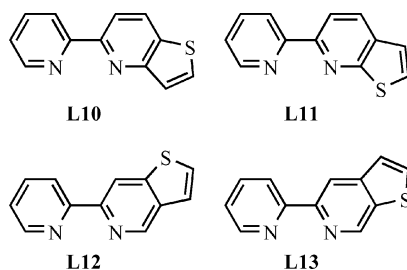
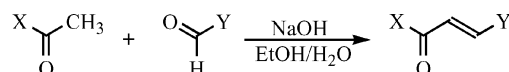


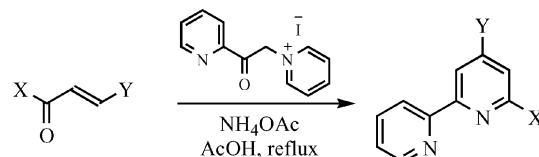
Figure 2. The fused thienopyridine ligands **L10–L13** used in this study.

The ligands **L1–L9** were prepared in moderate yields by adaptations of methods described earlier by Kröhnke^[6] and Constable.^[7] The propenone precursors (chalcones) **P2–P9** were generated by aldol condensation of the corresponding aromatic methyl ketone with an aromatic aldehyde (Scheme 1).



Scheme 1. The condensation reaction leading to the formation of the chalcone precursors **P2–P9** (X = H, thiophen-2-yl, 5-methylthiophen-2-yl; Y = thiophen-2-yl, 4-*tert*-butylphenyl, 4-methoxyphenyl, 4-nitrophenyl).

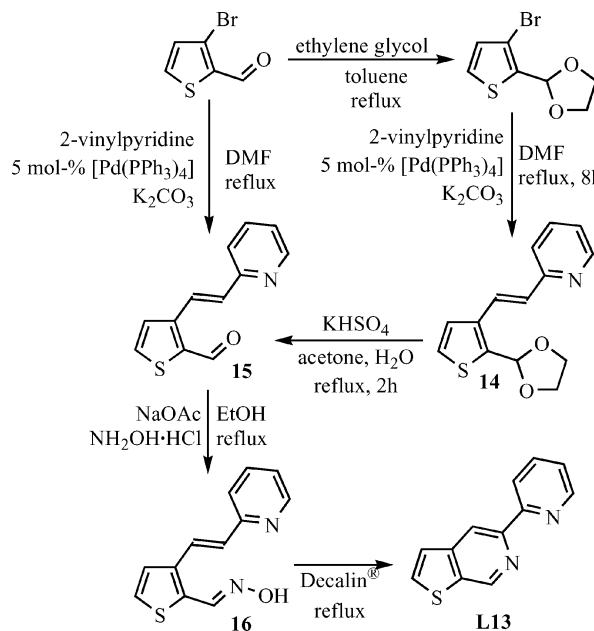
These chalcones were then treated with the Kröhnke reagent 2-[1-oxo-2-(1-pyridinio)ethyl]pyridine iodide^[6] and an excess of ammonium acetate (Scheme 2) to yield the pure products after column chromatography/Soxhlet extraction, and recrystallization.



Scheme 2. Generation of the 2,4,6-trisubstituted pyridines by using the Kröhnke methodology [X = H (**L2**), thiophen-2-yl (**L3–L5**), 5-methylthiophen-2-yl (**L6–L9**); Y = thiophen-2-yl (**L2**, **L9**), 4-*tert*-butylphenyl (**L3**, **L6**), 4-methoxyphenyl (**L4**, **L7**), 4-nitrophenyl (**L5**, **L8**)].

The fused pyridyl-thienopyridines **L10**, **L11** and **L12** were synthesized by using our recently reported methods,^[8] which are presented in schematic form in the Supporting Information (Schemes S1, S2 and S3, respectively).

The preparation of ligand **L13** began with an attempt to perform a Heck reaction on 3-bromothiophene-2-carbaldehyde (Scheme 3), but the reaction failed. Protection of the formyl group as a cyclic acetal^[9] (a functional group tolerated in the Heck reaction) resulted in subsequent formation of 2-{2-[2-(1,3-dioxolan-2-yl)thiophen-3-yl]vinyl}pyridine (**14**) in 94% yield. Steric effects could thereby be



Scheme 3. Synthetic route to 5-(pyridin-2-yl)thieno[2,3-*c*]pyridine (**L13**).

discounted as the reason for the failure of the Heck reaction in the earlier attempt, suggesting rather participation of formyl π -orbitals in the catalytic complex. Deprotection gave 3-[2-(pyridin-2-yl)vinyl]thiophene-2-carbaldehyde (**15**) in 87% yield, which could be quantitatively converted into the oxime **16** prior to the thermal ring-closure. The pyridyl-thienopyridine **L13** was then obtained in moderate yield by cyclization in Decalin® (35%).^[10]

Electrochemistry

The redox potentials of the Ru complexes determined by cyclic voltammetry in CH₃CN with 0.1 M Et₄NClO₄ as supporting electrolyte (reported in mV vs. the ferrocene/ferrocenium couple) are listed in Table 1. Three of these are shown in Figure 3 as representative of the compounds in this series. All voltammograms are collected in Figure S1 (Supporting Information), and were measured at a sweep rate of 200 mV s⁻¹. (Polypyridine)Ru^{II} complexes exhibit rich and complex electrochemistry in non-aqueous solutions comprising both metal-centred oxidation (Ru^{III/II}) and bpy-centred reduction reactions. The Ru^{III/II} couples are all totally reversible and appear in a narrow range (Table 1). The substitution of a thiophene ring into either the 4- or the 6-position of the 2,2'-bipyridine system appears to have only a minor effect upon the value for the Ru^{III/II} couple, with most complexes possessing values similar to that of the parent complex [Ru(bpy)₃]²⁺.

As the redox potentials displayed by the prototypes **C1** and **C2** fell within a narrow range, it was of interest to examine the effect on the Ru^{III/II} couple of a 4-Y-phenyl substituent upon the unique 2,2'-bipyridine ring system. For ease of synthesis, analogues of **L1** were chosen and the Kröhnke methodology^[6] applied, leading to the ligands **L3**–**L9** in moderate yields. The corresponding Ru^{III/II} couples for **C3**–**C9** were indeed found to reflect the electron-withdrawing/donating character of the Y substituent, but the shifts were small in all cases (1–33 mV). It is most likely that the transfer of electron density to and from the Y-sub-

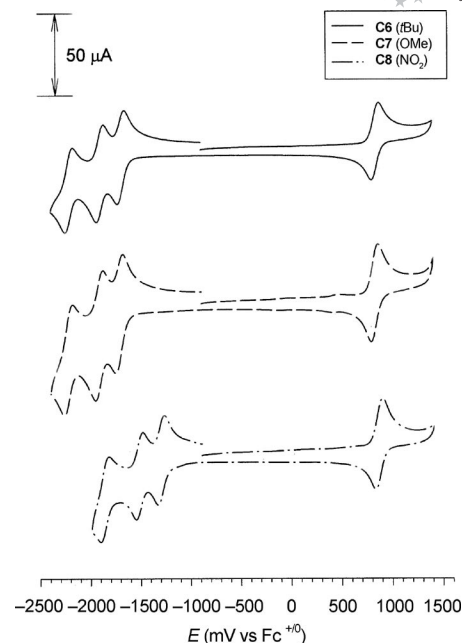


Figure 3. Voltammograms of the complexes **C6**, **C7** and **C8**. The concentration was 1 mM in CH₃CN, $\nu = 200 \text{ mV s}^{-1}$ and all other conditions are given in the Experimental Section.

stituent is abated by the inability of the phenyl ring to fully adopt a coplanar conformation with the central pyridine ring. The introduction of these Y-substituents directly onto one of the chelating rings to amplify their effect is currently under investigation.

The nitro group in **C5** and **C8** had a profound effect on the ligand-centred reduction potentials. The nitro group itself is electroactive and the distinctly different voltammetry displayed by these complexes (see Figure 3) is indicative of a reaction where reduction of the nitro-substituted bpy is facilitated by delocalisation over the nitro group. Interestingly, the second and third bpy reduction potentials are anodically shifted by a similar degree (Figure 3) indicating that electron delocalisation across the metal atom and the

Table 1. Redox potentials (mV vs. Fc^{+/0}). Experimental conditions: 1 mM complex in CH₃CN with 0.1 M Et₄NClO₄ as supporting electrolyte, $T = 298 \text{ K}$, glassy carbon working electrode (3 mm), Pt auxiliary electrode and Ag/Ag⁺ (MeCN) reference electrode, $\nu = 200 \text{ mV s}^{-1}$.

[Ru(bpy) ₂ L _n] ²⁺	[Ru(bpy) ₂ L _n] ^{3+/2+}	[Ru(bpy) ₂ L _n] ^{2+/+}	[Ru(bpy) ₂ L _n] ^{+/0}	[Ru(bpy) ₂ L _n] ^{0/-}
[Ru(bpy) ₃] ²⁺ ^[a]	+874	-1728	-1912	-2162
1	+869	-1706	-1915	-2227
2	+850	-1694	-1896	-2139
3	+854	-1690	-1899	-2215
4	+846	-1705	-1907	-2219
5	+878	-1295	-1514	-1890
6	+846	-1688	-1896	-2214
7	+836	-1706	-1908	-2216
8	+870	-1295	-1513	-1861
9	+845	-1653	-1889	-2208
10	+892	-1676	-1882	-2132
11	+924	-1641	-1874	-2136
12	+829	-1755	-1942	-2152
13	+849	-1758	-1948	-2214

[a] [Ru(bpy)₃]²⁺ data collected during this study.

three ligands influences all subsequent reductions. The presence of the 5-methylthiophen-2-yl substituent in **C6–C9** shifted the metal-centred oxidation to lower potentials, whereas the effects upon the ligand reductions were marginal.

The results for the fused pyridyl-thienopyridine complexes **C10–C13** were interesting and revealed some significant isomeric effects. The complexes in which the thiophene ring was fused to the *b* face of the bipyridine (**C10**, **C11**) exhibited higher $\text{Ru}^{\text{III/II}}$ potentials than $[\text{Ru}(\text{bpy})_3]^{2+}$, whereas those in which the thiophene was attached to the *c* face (**C12**, **C13**) were lower by a similar degree. The orientation of the fused thiophene ring (with the S-atom *syn* or *anti* relative to the adjacent N-donor) has an additional influence on the $\text{Ru}^{\text{III/II}}$ redox potential. In this case it seems that the proximity of the electronegative S-atom to the Ru ion is responsible for this effect. In compounds **C11** and **C13** the $\text{Ru}^{\text{III/II}}$ redox potential is ca. 20–30 mV higher than in **C10** and **C12**. The thiophene S-atoms in **C11** and **C13** are one connection closer to the Ru centre than **C10** and **C12**, respectively. The influences on the ligand-based reductions are less significant (see Table 1).

The rigid geometry of the ligands **L10** and **L11** can result in distortion of the inner coordination sphere of Ru, resulting in a poorer overlap between the donor atoms of the ligands and the $d\pi$ -orbitals of Ru, thus diminishing any electronic effect from the fused electron-rich thiophene ring. This, however, is not reflected in the luminescence results, as both **C10** and **C11** display red luminescence with a lifetime and intensity comparable to those of $[\text{Ru}(\text{bpy})_3]^{2+}$, compared with **C1** where only a very weak red luminescence is detected (see Table 2). The fusion of the thiophene ring onto the *c* face does not introduce the same steric strain to the inner coordination sphere, resulting in less positive $\text{Ru}^{\text{III}}/\text{Ru}^{\text{II}}$ couples and longer luminescence lifetimes (see next section). In our earlier work,^[5] a second oxidation process at higher potentials was detected in the voltammograms of complexes bearing a bithiophenyl moiety attached to one of the bpy ligands, whereas those possessing only a single (uncoupled) thiophene ring possessed no such wave. As anticipated, no such oxidation processes were observed for the complexes **C1–C13** within the solvent limit.

Table 2. Luminescence maxima, lifetimes and quantum yields for the Ru^{II} complexes **C1–C13**.

$[\text{Ru}(\text{bpy})_2\text{L}_n]^{2+}$	Luminescence peak [nm]	Quantum yield [ϕ]	τ [ns] ^[a]
$\text{Ru}(\text{bpy})_3^{2+}$	610	0.042 ^[11]	1745
C1	620	< 0.001	–
C2	610	0.045	3000
C3	620	< 0.001	–
C4–C9	–	–	–
C10	620	0.0047	275
C11	622	0.013	1040
C12	612	0.014	1420
C13	614	0.0097	1510

[a] Luminescence lifetimes at 610 nm, in CH_3CN under continuous Ar purge, 17.5 °C. In all cases excitation is at 337 nm from an N_2 laser.

Luminescence Properties

As observed in our previous study,^[5] the red $[\text{Ru}(\text{bpy})_3]^{2+}$ -type MLCT luminescence was quenched in those cases where a thiophenyl substituent was present in the 6-position of the unique 2,2'-bipyridine, the only exception being the prototype **C1** and **C3** where a very weak red luminescence was observed (see Table 2). Whereas, when the thiophene is attached to the 4-position (**C2**), a red luminescence and an excitation spectrum very similar to that of $[\text{Ru}(\text{bpy})_3]^{2+}$ (Figure 4) are observed, although with a slightly greater quantum yield and longer lifetime (3000 ns) when compared to that of $[\text{Ru}(\text{bpy})_3]^{2+}$ (1745 ns) obtained under identical conditions.

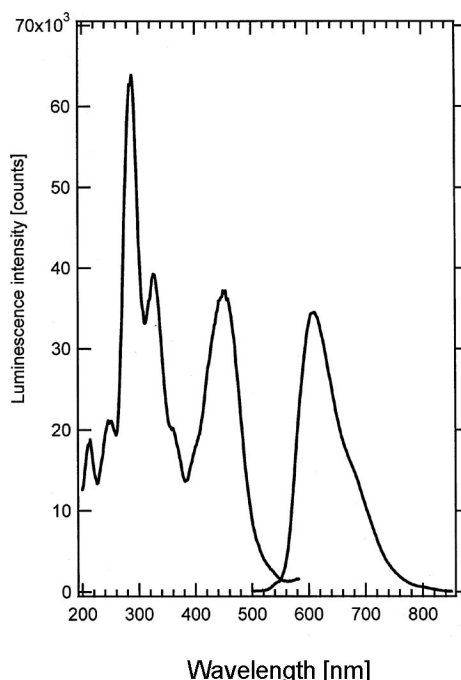


Figure 4. Luminescence (RHS, $\lambda_{\text{ex}} = 337$ nm) and excitation (LHS, $\lambda_{\text{em}} = 410$ nm) spectra of **C2** in CH_3CN solution.

The red luminescence spectra observed for complexes **C2** and **C10–C13** were similar to that of $[\text{Ru}(\text{bpy})_3]^{2+}$ with small wavelength shifts, and the luminescence band maxima, quantum yield and lifetimes are given in Table 2. The same emission spectra are observed when excited at either 337 or 450 nm. All excitation spectra indicate that the complexes have similar excited state structures, whereas the similarity in shape, lifetime and excitation maxima of the emission indicates that for these complexes it originates from the same $^3\text{MLCT}$ transition.

The weak red luminescence observed in complexes **C1** and **C3** was only detected in freshly prepared solutions. The luminescence becomes weaker over time, disappearing after several hours. It has been previously reported that photolysis of $[\text{Ru}(\text{bpy})_3]^{2+}$ results in loss of one bpy ligand;^[11] furthermore, it has been shown that in acetonitrile solutions the formation of CH_3CN -coordinated bis(bpy)ruthenium(II) complexes can occur.^[12] Analysis by ^1H NMR spectroscopy of CD_3CN solutions of **C1** and **C3** indicated

that under the influence of ambient light photosubstitution occurs, and the complex $[\text{Ru}(\text{bpy})_2(\text{CD}_3\text{CN})_2]^{2+}$ is formed,^[13a–13c] with subsequent loss of luminescence. For the complexes **C4–C9**, the red luminescence was completely absent.

In the complexes where the red luminescence is weak (**C1**, **C3**) or absent and the ligand does not contain a nitro group (**C4**, **C6**, **C7**, **C9**) a blue emission characteristic of the free ligand is observed. The origin of this blue emission is unlikely to be a ligand-centred (LC) emission of the complex, as the lifetimes are very short (< 10 ns) implying a spin-allowed fluorescence, unlike the ^3LC emission detected, for example, in $[\text{Ru}(\text{i-biq})_3]^{2+}$ (i-biq = 3,3'-biisoquinoline).^[14] In addition the observed blue emission of these complexes is unshifted with respect to that of the pure ligand, and has identical excitation spectra. We conclude that this ligand emission is either due to small amounts of ligand impurity in our samples, or that some ligand dissociation is occurring. For the complexes containing the nitro group (**C5** and **C8**) neither blue nor red emission was observed.

A comparison of the excitation and emission spectra of the four fused pyridyl-thienopyridine complexes **C10–C13** is displayed in Figure 5. The lifetimes for **C10–C13** are somewhat shorter than those observed for $[\text{Ru}(\text{bpy})_3]^{2+}$ and the prototypic **C2** under the same conditions. These four red luminescent compounds are all isomers, and the differences in the luminescence lifetimes may be due to the different accessibility of the C–H vibrations to the emission process, which would promote radiationless relaxation.

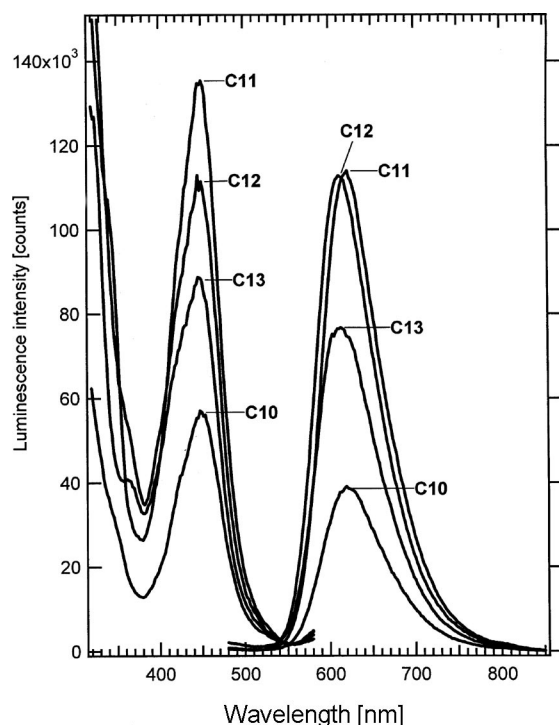


Figure 5. Luminescence ($\lambda_{\text{ex}} = 337$ nm) and excitation spectra of **C10–C13** in CH_3CN . The excitation spectra were measured by monitoring the luminescence intensity of the peak position of the luminescence spectra.

In addition, the luminescence of **C10** and **C11** is slightly redshifted with respect to **C12** and **C13** (Figure 5 and Table 2) which may indicate that the filled t_{2g} metal orbitals are shifted to higher energy, decreasing the energy of the MLCT transition. The luminescence spectra in Figure 5 were recorded at concentrations that gave the same absorption at the 337 nm excitation wavelength in order to quantify the quantum yield (Table 2). The quantum yields of the complexes **C10–C13** were somewhat smaller than that of $[\text{Ru}(\text{bpy})_3]^{2+}$, with that of **C10** being the smallest. However, all complexes with fused thiophene were markedly different from the non-luminescent complexes with the thiophene at the 6-position, **C3–C9**.

Conclusions

The excited-state lifetimes were found to correlate strongly with the structure of the chelating bipyridine unit; thus, both the position and mode of attachment have important consequences for the establishment of a stable excited electronic state. If the unique ligand possessed a thiophene substituent in the 6-position of the 2,2'-bipyridine (motif **L1**) luminescence was very weak or absent.

The deactivation of luminescence from complexes with 6-substituted bipyridyl ligands is well known^[16,3a] and has been rationalized by a decrease in the energy gap between the $^3\text{MLCT}$ and a higher metal-centred state (^3MC) based on ligand-field transitions to the σ^* -orbitals. The ^3MC state is expected to have a large geometry change from the ground state and provides an efficient pathway for radiationless relaxation. This mechanism has been used to explain the weak luminescence of bis(terpyridine) Ru^{II} where the ^3MC state is lowered due to a weaker ligand field from the small bite angle of the terpyridine ligand.^[16] A distortion in the coordination geometry from octahedral geometry is also thought to lower the ^3MC state. In the present case, presumably it is the distortion due to steric factors between the pendant 6-thiophen-2-yl substituent and an adjacent bipyridine auxiliary ligand that leads to deactivation of the luminescence and the long-lived excited state desired for electron transfer.

When the thiophene ring is moved to the 4-position (and the 6-position is unsubstituted, motif **L2**), red luminescence is observed with a higher quantum efficiency and a longer lifetime than those of $[\text{Ru}(\text{bpy})_3]^{2+}$ (see Table 2). The fusion of the thiophene ring onto either the *b* or *c* face of one of the pyridine rings, thereby ensuring a completely planar interface between the chelator and the conjugation-extending thiophene ring, led to a series of ligands **L10–L13**, the complexes of which all displayed red luminescence with lifetimes slightly shorter than that of $[\text{Ru}(\text{bpy})_3]^{2+}$. Fusions to the *b* and *c* faces were chosen so as to achieve both a non-charged thienopyridine (a charged system would result from fusion to the *a* face) and to avoid steric interactions within the interannular region of the bipyridine. Those complexes which contained a fused thiophene on the *c* face (**C12** and **C13**) displayed the longest lifetimes in this series,

in line with the fact that their coordination geometries most closely mimic that of $[\text{Ru}(\text{bpy})_3]^{2+}$. As only weak electronic coupling was found in bridged dimetallic complexes comprising the chelating motifs **L1** and **L2**,^[5] it is therefore of interest to extend these studies through the generation of bridged complexes by utilising the fused **L12** and **L13** motifs. The study of the photophysical properties and intervalence charge-transfer properties (IVCT) of such bridged complexes will help elucidate the optimal structural and electronic requirements for communication between metal centres linked in this manner.

Experimental Section

General: All moisture- and air-sensitive reactions were performed in oven-dried (120 °C, 12 h) glassware under nitrogen. Analytical TLC was performed on commercially prepared plates coated with 0.20 mm of Macherey–Nagel silica gel 60. The compounds were visualized by illumination with UV light (254 nm). Column chromatography was performed by using Matrex Normal Phase Silica 60 (particle size 35–70 μm). All melting points were determined by using an Electrothermal 9200 melting point apparatus and are uncorrected. Infrared spectra (IR) were measured with a Perkin–Elmer Spectrum One spectrophotometer. Mass spectra (MS) were obtained with a Fisons Instrument Trio 1000 spectrometer equipped with a Hewlett Packard 5MS GC column. NMR spectra were recorded with a Bruker DPX Avance 300 MHz spectrometer, and the chemical shifts are expressed in ppm from tetramethylsilane as internal standard. Abbreviations for signal coupling are as follows: s, singlet; d, doublet; t, triplet; q, quartet; dd, doublet of doublets; ddd, doublet of doublets of doublets; dt, doublet of triplets; m, multiplet; br., broad. All commercially available chemicals were used as received unless otherwise noted. Steady-state luminescence spectra were acquired with an ISS PC1 fluorimeter in photon-counting mode immediately after purging with argon gas. Concentrations were adjusted to give an absorption of 0.05 at the excitation wavelength of 337 nm, and were in the range $1\text{--}3 \times 10^{-6}$ M. Luminescence lifetimes were measured by using the 337 nm excitation of an N_2 laser at 2 Hz. After a long-pass filter and Jobin Yvon H-20 monochromator centred at 610 nm, the luminescence was detected by an S-20 photomultiplier tube. The signal was amplified by two stages of a Stanford 445 preamplifier and collected with a Tektronix TDS4010 digital storage oscilloscope. The solutions were purged with argon for 20 min before and during the lifetime measurements. The red-emitting compounds show a strong sensitivity to dissolved oxygen. All luminescence measurements were carried out with acetonitrile solutions at 17.5 °C. Quantum efficiency measurements were obtained from integrating the spectra when plotted in wavenumber, adjusting for the refractive index of acetonitrile and using the value of $\phi = 0.042$ for $[\text{Ru}(\text{bpy})_3]^{2+}$ as a standard.^[15,17] The error in the measurements were as follows; luminescence peak ± 1 nm; quantum yield $\pm 10\%$; luminescence lifetimes ± 10 ns. Cyclic voltammetry was performed with a BAS100B/W electrochemical workstation by employing a glassy carbon working electrode (3 mm), an Ag/Ag^+ (MeCN) non-aqueous reference electrode and a Pt wire counter electrode. All solutions contained ca. 1 mM complex in CH_3CN , and the supporting electrolyte was Et_4NClO_4 . The electrochemical cell was purged with nitrogen before measurement and maintained anaerobic during measurement with a blanket of nitrogen. All potentials are cited relative to the ferrocene/ferrocenium redox couple [measured here

as +87 mV vs. $\text{Ag}/\text{Ag}^+(\text{MeCN})$]. The potentials are correct to a precision of ± 5 mV.

Synthetic Procedures

Representative Procedure for the Preparation of the Complexes from Their Corresponding Ligands

$[\text{Ru}(\text{bpy})_2(\text{L3})]$ (C3): Ligand **L3** (74.1 mg, 200 μmol) and $\text{Ru}(\text{bpy})_2\text{Cl}_2$ (96.6 mg, 200 μmol) were dissolved in ethylene glycol (6 mL) and heated to 120 °C. After 2 h, TLC showed complete consumption of the ligand, and heating was stopped. When the mixture reached room temp., a solution of ammonium hexafluorophosphate (97.8 mg, 600 μmol) in H_2O (16 mL) was added. The mixture was placed in a refrigerator overnight and then cooled in ice to complete precipitation. The red precipitate was collected on a sintered glass funnel and was purified by dissolution in the minimum amount of CH_3CN and addition to diethyl ether (200 mL). The red precipitate was recovered by suction filtration and reprecipitated a second time. The product was recovered by suction filtration through a fine glass funnel. Analytical samples were prepared by recrystallization from CH_3CN or dichloromethane. Product appearance: orange/red powder. Yield: 193 mg (90%). ^1H NMR ($[\text{D}_6]\text{dmsO}$, 300 MHz): δ = 9.22 (d, J = 8.0 Hz, 1 H), 9.15 (s, 1 H), 8.82 (d, J = 8.3 Hz, 1 H), 8.77–8.68 (m, 2 H), 8.51 (d, J = 5.6 Hz, 1 H), 8.39 (d, J = 8.2 Hz, 1 H), 8.28–8.14 (m, 3 H), 8.10–8.01 (m, 3 H), 7.86 (d, J = 1.4 Hz, 1 H), 7.80–7.68 (m, 2 H), 7.67–7.54 (m, 4 H), 7.54–7.43 (m, 2 H), 7.43–7.31 (m, 2 H), 7.22 (d, J = 4.9 Hz, 1 H), 7.09–6.95 (m, 2 H), 6.45 (br. s, 1 H), 1.32 (s, 9 H) ppm. $\text{C}_{44}\text{H}_{38}\text{F}_{12}\text{N}_6\text{P}_2\text{RuS}$ (1073.89) + 4 H_2O + 1/2 CH_3CN : calcd. C 46.34, H 4.10, N 7.81; found C 46.24, H 3.97, N 7.78.

$[\text{Ru}(\text{bpy})_2(\text{L1})]$ (C1): Orange/red powder (75%). ^1H NMR (CD_3CN , 300 MHz): δ = 8.59 (m, 2 H), 8.48 (d, 1 H), 8.42 (d, 1 H), 8.40 (d, 1 H), 8.31 (dm, 1 H), 8.11 (td, 1 H), 8.10 (d, 1 H), 8.09 (m, 2 H), 8.08 (td, 1 H), 7.94 (td, 1 H), 7.70 (dm, 1 H), 7.65 (td, 1 H), 7.56 (dm, 1 H), 7.52 (m, 1 H), 7.48 (d, 1 H), 7.39 (dm, 1 H), 7.38 (m, 1 H), 7.33 (m, 1 H), 7.21 (m, 1 H), 7.11 (dm, 1 H), 7.04 (d, 1 H), 6.89 (m, 1 H), 6.40 (m, 1 H) ppm. $\text{C}_{34}\text{H}_{26}\text{F}_{12}\text{N}_6\text{P}_2\text{RuS}$ (941.69) + 1/3 CH_2Cl_2 : calcd. C 42.51, H 2.77, N 8.66; found C 42.74, H 2.92, N 8.57. MS (MALDI-TOF): m/z (calcd.) = 653 (651.7) $[\text{M} + \text{H} - 2 \text{PF}_6]^+$.

$[\text{Ru}(\text{bpy})_2(\text{L2})]$ (C2): Orange/red powder (81%). ^1H NMR (CD_3CN , 300 MHz): δ = 8.68 (d, 1 H), 8.65 (s, 1 H), 8.47–8.53 (d, 4 H), 8.08 (td, 1 H), 8.03–8.10 (td, 4 H), 7.90 (dd, 1 H), 7.76 (dm, 1 H), 7.84 (dm, 4 H), 7.71 (dd, 1 H), 7.64 (d, 1 H), 7.56 (d, 1 H), 7.42 (m, 1 H), 7.37–7.45 (m, 4 H), 7.27 (m, 1 H) ppm. $\text{C}_{34}\text{H}_{26}\text{F}_{12}\text{N}_6\text{P}_2\text{RuS}$ (941.69) + 1/3 CH_2Cl_2 : calcd. C 42.51, H 2.77, N 8.66; found C 42.59, H 2.83, N 8.45. MALDI-TOF MS: m/z (calcd.) = 796 (796.7) $[\text{M} - \text{PF}_6]^+$, 652 (651.7) $[\text{M} - 2 \text{PF}_6]^+$.

$[\text{Ru}(\text{bpy})_2(\text{L4})]$ (C4): Orange/red powder (85%). ^1H NMR (CD_3CN , 300 MHz): δ = 8.79–8.74 (m, 2 H), 8.49–8.31 (m, 4 H), 8.14–8.04 (m, 4 H), 7.97–7.89 (m, 3 H), 7.74–7.70 (m, 2 H), 7.65 (dt, J = 1.4, 7.9 Hz, 1 H), 7.58–7.48 (m, 2 H), 7.42–7.30 (m, 3 H), 7.22 (ddd, J = 1.2, 5.7, 7.6 Hz, 1 H), 7.16–7.08 (m, 3 H), 7.03 (d, J = 5.4 Hz, 1 H), 6.87 (ddd, J = 1.2, 5.7, 7.6 Hz, 1 H), 6.40 (t, J = 3.9 Hz, 1 H), 3.88 (s, 3 H) ppm. $\text{C}_{41}\text{H}_{32}\text{F}_{12}\text{N}_6\text{OP}_2\text{RuS}$ (1047.81) + 2 H_2O : calcd. C 45.44, H 3.35, N 7.75; found C 45.55, H 3.48, N 7.71. MALDI-TOF MS: m/z (calcd.) = 901.9 (901.9) $[\text{M} - \text{H} - \text{PF}_6]^+$, 756.0 (755.9) $[\text{M} - 2 \text{H} - 2 \text{PF}_6]^+$.

$[\text{Ru}(\text{bpy})_2(\text{L5})]$ (C5): Orange/red powder (89%). ^1H NMR (CD_3CN , 300 MHz): δ = 8.86 (d, J = 1.9 Hz, 1 H), 8.79 (d, J = 8.1 Hz, 1 H), 8.52–8.35 (m, 5 H), 8.32 (d, J = 5.3 Hz, 1 H), 8.18–8.05 (m, 6 H), 7.95 (dt, J = 1.4, 7.9 Hz, 1 H), 7.81 (d, J = 1.9 Hz, 1 H), 7.75–7.48 (m, 4 H), 7.45–7.32 (m, 3 H), 7.23 (dt, J = 1.2, 7.0 Hz, 1 H), 7.12

(d, $J = 5.1$ Hz, 1 H), 7.05 (d, $J = 4.9$ Hz, 1 H), 6.89 (t, $J = 6.1$ Hz, 1 H), 6.41 (br. t, 1 H) ppm. $C_{40}H_{29}F_{12}N_7O_2P_2RuS$ (1062.78): calcd. C 45.21, H 2.71, N 9.23; found C 45.09, H 2.89, N 8.95.

[Ru(bpy)₂(L6)] (C6): Orange/red powder (70%). ¹H NMR (CD_3CN , 300 MHz): $\delta = 8.79$ (d, $J = 2.0$ Hz, 1 H), 8.76 (d, $J = 8.2$ Hz), 8.50–8.35 (m, 3 H), 8.25 (d, $J = 5.5$ Hz, 1 H), 8.14–8.05 (m, 4 H), 8.95 (dt, $J = 1.4$, 7.9 Hz, 1 H), 7.89 (d, $J = 8.6$ Hz, 2 H), 7.77 (d, $J = 2.0$ Hz, 1 H), 7.75–7.67 (m, 2 H), 7.64 (d, $J = 8.6$ Hz, 2 H), 7.57 (d, $J = 5.6$ Hz, 1 H), 7.51 (ddd, $J = 1.2$, 5.7, 7.6 Hz, 1 H), 7.44–7.30 (m, 3 H), 7.23 (ddd, $J = 1.3$, 5.7, 7.6 Hz), 7.18 (d, $J = 5.6$ Hz, 1 H), 6.95 (ddd, $J = 1.2$, 5.7, 7.6 Hz, 1 H), 6.5–5.7 (br. m, 2 H), 2.18 (s, 3 H), 1.37 (s, 9 H) ppm. $C_{45}H_{40}F_{12}N_6P_2RuS$ (1087.92) + 2 H₂O: calcd. C 48.09, H 3.95, N 7.48; found C 48.31, H 3.48, N 7.51. MALDI-TOF MS: m/z (calcd.) = 941.9 (942.1) [M – 2 H – PF₆]⁺.

[Ru(bpy)₂(L7)] (C7): Orange/red powder (35%). ¹H NMR (CD_3CN , 300 MHz): $\delta = 8.78$ –8.72 (m, 2 H), 8.50–8.36 (m, 3 H), 8.28 (d, $J = 5.1$ Hz, 1 H), 8.13–8.04 (m, 4 H), 8.00–7.88 (m, 3 H), 7.74–7.66 (m, 3 H), 7.56 (d, $J = 5.0$ Hz, 1 H), 7.50 (ddd, $J = 1.2$, 5.7, 7.6 Hz, 1 H), 7.43–7.29 (m, 3 H), 7.26–7.09 (m, 4 H), 6.94 (ddd, $J = 1.2$, 6.0, 7.2 Hz, 1 H), 6.5–5.7 (br. m, 2 H), 3.88 (s, 3 H), 2.18 (s, 3 H) ppm. $C_{42}H_{34}F_{12}N_6OP_2RuS$ (1045.84) + 1/2 H₂O: calcd. C 47.11, H 3.29, N 7.85; found C 46.83, H 2.89, N 7.84.

[Ru(bpy)₂(L8)] (C8): Red/brown powder (79%). ¹H NMR (CD_3CN , 300 MHz): $\delta = 8.83$ (d, $J = 2.1$ Hz, 1 H), 8.77 (d, $J = 8.2$ Hz, 1 H), 8.50–8.37 (m, 5 H), 8.25 (d, $J = 5.6$ Hz, 1 H), 8.15–8.05 (m, 6 H), 7.96 (dt, $J = 1.5$, 7.9 Hz, 1 H), 7.81 (d, $J = 2.0$ Hz, 1 H), 7.75–7.67 (m, 2 H), 7.58 (d, $J = 5.7$ Hz, 1 H), 7.51 (ddd, $J = 1.3$, 5.7, 7.6 Hz, 1 H), 7.43–7.32 (m, 3 H), 7.26 (ddd, $J = 1.3$, 5.7, 7.6 Hz, 1 H), 7.17 (d, $J = 5.6$ Hz, 1 H), 6.95 (ddd, $J = 1.3$, 5.6, 7.6 Hz, 1 H), 6.5–5.7 (br. m, 2 H), 2.18 (s, 3 H) ppm. $C_{41}H_{31}F_{12}N_7O_2P_2RuS$ (1076.81) + 1/2 H₂O: calcd. C 45.35, H 2.97, N 9.03; found C 45.08, H 2.58, N 9.02. MALDI-TOF MS: m/z (calcd.) = 785.2 (785.2) [M – H – PF₆]⁺.

[Ru(bpy)₂(L9)] (C9): Orange/red powder (64%). ¹H NMR (CD_3CN , 300 MHz): $\delta = 8.74$ (d, $J = 8.2$ Hz, 1 H), 8.67 (d, $J = 2.1$ Hz, 1 H), 8.50–8.35 (m, 3 H), 8.30 (d, $J = 5.6$ Hz, 1 H), 8.15–8.04 (m, 4 H), 7.98–7.91 (m, 2 H), 7.76–7.65 (m, 4 H), 7.56 (d, $J = 5.6$ Hz, 1 H), 7.51 (ddd, $J = 1.2$, 5.7, 7.6 Hz, 1 H), 7.43–7.30 (m, 3 H), 7.27 (dd, $J = 3.8$, 5.0 Hz, 1 H), 7.22 (ddd, $J = 1.2$, 5.7, 7.6 Hz, 1 H), 7.16 (d, $J = 5.6$ Hz, 1 H), 6.95 (ddd, $J = 1.2$, 5.7, 7.6 Hz, 1 H), 6.6–5.3 (br. m, 2 H), 2.18 (s, 3 H) ppm. $C_{39}H_{30}F_{12}N_6P_2RuS_2$ (1051.84) + 1 H₂O: calcd. C 44.36, H 3.05, N 7.96; found C 44.11, H 2.68, N 7.68. MALDI-TOF MS: m/z (calcd.) = 891.9 (891.9) [M – H – PF₆]⁺, 746.0 (746.0) [M – 2 H – 2 PF₆]⁺.

[Ru(bpy)₂(L10)] (C10): Orange/red powder (78%). ¹H NMR (CD_3CN , 300 MHz): $\delta = 8.68$ (dd, $J = 8.7$, 0.75 Hz, 1 H), 8.64 (d, $J = 8.2$ Hz, 1 H), 8.69–8.47 (m, 4 H), 8.44 (d, $J = 8.1$ Hz, 1 H), 8.14–8.05 (m, 4 H), 8.00 (dt, $J = 1.4$, 7.9 Hz, 1 H), 7.92–7.85 (m, 2 H), 7.81 (d, $J = 5.81$ Hz, 1 H), 7.67–7.60 (m, 3 H), 7.46 (ddd, $J = 1.4$, 5.7, 7.5 Hz, 1 H), 7.42–7.31 (m, 4 H), 6.12 (dd, $J = 5.8$, 0.75 Hz, 1 H) ppm. $C_{32}H_{24}F_{12}N_6P_2RuS$ (915.65) + 1/2 H₂O: calcd. C 41.57, H 2.73, N 9.09; found C 41.21, H 2.35, N 8.92. MALDI-TOF MS: m/z (calcd.) = 770.7 (770.7) [M – PF₆]⁺, 625.5 (625.7) [M – 2 PF₆]⁺.

[Ru(bpy)₂(L11)] (C11): Orange/red powder (93%). ¹H NMR (CD_3CN , 300 MHz): $\delta = 8.61$ (d, $J = 8.2$ Hz, 1 H), 8.58–8.43 (m, 6 H), 8.12–7.98 (m, 5 H), 7.84 (d, $J = 5.6$ Hz, 1 H), 7.74 (d, $J = 5.6$ Hz, 1 H), 7.68–7.60 (m, 3 H), 7.52 (d, $J = 6.0$ Hz, 1 H), 7.47 (d, $J = 6.0$ Hz, 1 H), 7.43–7.29 (m, 5 H) ppm. $C_{32}H_{24}F_{12}N_6P_2RuS$ (915.45): calcd. C 41.98, H 2.64, N 9.18; found C 41.80, H 2.22, N 9.18. MALDI-TOF MS: m/z (calcd.) = 770.7 (770.7) [M – PF₆]⁺, 625.5 (625.8) [M – 2 PF₆]⁺.

[Ru(bpy)₂(L12)] (C12): Orange/red powder (95%). ¹H NMR (CD_3CN , 300 MHz): $\delta = 9.15$ (s, 1 H), 8.54–8.44 (m, 5 H), 8.25 (d, $J = 0.44$ Hz, 1 H), 8.11–7.98 (m, 5 H), 7.93 (d, $J = 5.5$ Hz, 1 H), 7.81–7.67 (m, 5 H), 7.45–7.31 (m, 6 H) ppm. $C_{32}H_{24}F_{12}N_6P_2RuS$ (915.65) + 2 H₂O: calcd. C 40.39, H 2.97, N 8.83; found C 40.64, H 2.58, N 8.66. MALDI-TOF MS: m/z (calcd.) = 770.7 (770.7) [M – PF₆]⁺, 625.5 (625.8) [M – 2 PF₆]⁺.

[Ru(bpy)₂(L13)] (C13): Orange/red powder (60%). ¹H NMR (CD_3CN , 300 MHz): $\delta = 9.01$ (s, 1 H), 8.56–8.49 (m, 5 H), 8.39 (s, 1 H), 8.12 (d, $J = 5.4$ Hz, 1 H), 8.12–8.01 (m, 5 H), 7.83–7.73 (m, 5 H), 7.71 (d, $J = 5.4$ Hz, 1 H), 7.45–7.33 (m, 5 H) ppm. $C_{32}H_{24}F_{12}N_6P_2RuS$ (915.65) + 1 H₂O: calcd. C 41.17, H 2.81, N 9.00; found C 41.09, H 2.82, N 8.90. MALDI-TOF MS: m/z (calcd.) = 769.7 (769.7) [M – H – PF₆]⁺, 624.8 (624.8) [M – H – 2 PF₆]⁺.

Preparation of Ligand L1

6-(Thiophen-2-yl)-2,2'-bipyridine (L1): This compound was prepared according to the method of Constable, Henney and Leese.^[7] Yield: 65%. M.p. 78 °C (ref.^[6,10] 78 °C). FT-IR: $\tilde{\nu} = 3051$ (w), 1578 (m), 1561 (s), 1530 (m), 1475 (m), 1454 (s), 1425 (s), 1349 (w), 1311 (w), 1290 (w), 1268 (w), 1227 (w), 1152 (m), 1091 (w), 1079 (m), 1045 (w), 996 (m), 967 (w), 905 (w), 852 (m), 825 (w), 778 (s), 746 (w), 737 (w), 717 (s), 689 (m), 652 (w), 625 (m), 569 (w), 508 (w) cm^{-1} . ¹H NMR ($CDCl_3$, 300 MHz): $\delta = 8.68$ (br. d, 1 H), 8.58 (d, $J = 7.8$ Hz, 1 H), 8.29 (dd, $J = 1.0$, 7.8 Hz, 1 H), 7.85 (dt, $J = 2.0$, 7.8 Hz, 1 H), 7.81 (t, $J = 7.8$ Hz, 1 H), 7.66 (dd, $J = 1.0$, 7.8 Hz, 1 H), 7.65 (dd, $J = 1.0$, 3.4 Hz, 1 H), 7.42 (dd, $J = 1.0$, 4.9 Hz, 1 H), 7.29–7.34 (m, 1 H), 7.13 (dd, $J = 3.4$, 4.9 Hz, 1 H) ppm.

Representative Procedure for the Preparation of Ligands L2–L9

4-(4-tert-Butylphenyl)-6-(thiophen-2-yl)-2,2'-bipyridine (L3): Propenone **P3** (2.70 g, 10 mmol), 2-[1-oxo-2-(1-pyridinio)ethyl]pyridine iodide^[6] (3.26 g, 10 mmol) and ammonium acetate (3.85 g, 50 mmol) were dissolved in glacial acetic acid (40 mL) and refluxed for 4 h. The reaction mixture was cooled to room temperature and then in ice before being rendered alkaline with NaOH and then extracted with dichloromethane (3 × 50 mL). The collected organic phases were washed with water (50 mL) and brine (50 mL) and dried with MgSO₄. After evaporation of the solvent, a black oil was obtained, which was purified by column chromatography with an EtOAc/hexane (1:6) eluent system. The product glows intensely blue upon radiation at 356 nm on a TLC plate. Recrystallization from methanol gave a pure product. Product appearance: yellow crystals. Yield: 1.15 g (31%). M.p. 129.7–131.2 °C. FT-IR: $\tilde{\nu} = 2962$ (m), 1600 (s), 1583 (s), 1567 (m), 1542 (s), 1473 (m), 1434 (w), 1388 (m), 830 (s), 793 (s), 743 (w), 699 (s), 540 (w) cm^{-1} . ¹H NMR (300 MHz, $CDCl_3$): $\delta = 8.73$ (d, $J = 4.1$ Hz, 1 H), 8.66 (d, $J = 8.0$ Hz, 1 H), 8.63 (s, 1 H), 7.95–7.86 (m, 2 H), 7.78 (d, $J = 8.4$ Hz, 1 H), 7.73 (dd, $J = 1.1$, 3.7 Hz, 1 H), 7.54 (d, $J = 8.4$ Hz, 1 H), 7.43 (dd, $J = 1.1$, 5.1 Hz, 1 H), 7.38 (ddd, $J = 0.9$, 5.1, 7.1 Hz, 1 H), 7.16 (dd, $J = 3.7$, 5.1 Hz, 1 H), 1.38 (s, 9 H) ppm. ¹³C NMR ($CDCl_3$, 75 MHz): $\delta = 156.2$, 155.9, 152.8, 152.7, 150.4, 149.1, 145.7, 137.7, 135.8, 128.4, 128.0, 127.4, 125.0, 124.3, 122.1, 117.7, 117.1, 35.2, 31.8 ppm.

4-(Thiophen-2-yl)-2,2'-bipyridine (L2): Pale yellow prisms (44%). M.p. 106–107.5 °C. FT-IR: $\tilde{\nu} = 3074$ (w), 3048 (w), 2999 (w), 1598 (s), 1580 (s), 1563 (s), 1547 (s), 1522 (m), 1457 (s), 1424 (m), 1395 (s), 1357 (w), 1345 (w), 1286 (w), 1270 (w), 1256 (w), 1233 (w), 1196 (w), 1151 (w), 1094 (w), 1054 (w), 990 (m), 910 (w), 891 (w), 855 (w), 823 (w), 795 (s), 741 (w), 700 (s), 659 (w), 637 (w), 617 (w) cm^{-1} . ¹H NMR ($CDCl_3$, 300 MHz): $\delta = 8.73$ (m, $J = 4.8$, 0.9 Hz, 1 H), 8.69–8.64 (m, 2 H), 8.44 (d, $J = 8.0$ Hz, 1 H), 7.85 (dt, $J = 7.8$,

1.8 Hz, 1 H), 7.67 (dd, $J = 3.7$, 1.1 Hz, 1 H), 7.53 (dd, $J = 5.2$, 1.9 Hz, 1 H), 7.45 (dd, $J = 5.1$, 1.1 Hz, 1 H), 7.36 (ddd, $J = 7.5$, 3.6, 1.2 Hz, 1 H), 7.17 (dd, $J = 5.1$, 3.6 Hz, 1 H) ppm. ^{13}C NMR (CDCl_3 , 75 MHz): $\delta = 157.0$, 156.1, 150.0, 149.4, 142.6, 141.7, 137.2, 128.6, 127.4, 125.8, 124.1, 121.5, 120.1, 117.4 ppm.

4-(4-Methoxyphenyl)-6-(thiophen-2-yl)-2,2'-bipyridine (L4): Yellow crystals (51%). M.p. 145.9–147.3 °C. FT-IR: $\tilde{\nu} = 1598$ (m), 1582 (m), 1568 (w), 1543 (w), 1515 (s), 1472 (w), 1424 (w), 1391 (w), 1295 (w), 1257 (m), 1183 (w), 1110 (w), 1032 (w), 829 (m), 795 (m), 714 (m), 575 (w), 513 (w) cm^{-1} . ^1H NMR (CDCl_3 , 300 MHz): $\delta = 8.72$ (d, $J = 0.8$, 4.8 Hz, 1 H), 8.64 (d, $J = 8.0$ Hz, 1 H), 8.55 (d, $J = 1.2$ Hz, 1 H), 7.88 (dt, $J = 1.6$, 8.0 Hz, 1 H), 7.85 (d, $J = 1.5$ Hz, 1 H), 7.78 (d, $J = 8.8$ Hz, 2 H), 7.73 (dd, $J = 1.0$, 3.7 Hz, 1 H), 7.44 (dd, $J = 1.0$, 5.0 Hz, 1 H), 7.34 (ddd, $J = 0.8$, 7.3, 4.9 Hz, 1 H), 7.17 (dd, $J = 3.7$, 5.0 Hz, 1 H), 7.04 (d, $J = 8.8$ Hz, 2 H), 3.89 (s, 9 H) ppm. ^{13}C NMR (CDCl_3 , 75 MHz): $\delta = 160.9$, 156.4, 152.7, 150.1, 149.4, 145.9, 137.4, 131.1, 128.8, 128.4, 128.0, 124.9, 124.3, 122.0, 117.1, 116.5, 114.8, 55.8 ppm.

4-(4-Nitrophenyl)-6-(thiophen-2-yl)-2,2'-bipyridine (L5): Green crystals (28%). M.p. 167.4–169.4 °C (ref.^[6] 183 °C). FT-IR: $\tilde{\nu} = 3110$ (w), 3087 (w), 1651 (w), 1595 (m), 1581 (m), 1548 (m), 1511 (s), 1472 (w), 1435 (w), 1419 (w), 1387 (w), 1346 (s), 1242 (w), 1110 (w), 859 (w), 851 (m), 793 (w), 780 (w), 755 (m), 742 (w), 689 (m) cm^{-1} . ^1H NMR ($[\text{D}_6]\text{dmsO}$, 300 MHz): $\delta = 8.74$ (d, $J = 4.5$ Hz, 1 H), 8.56 (s, 1 H), 8.48 (d, $J = 7.9$ Hz, 1 H), 8.39 (d, $J = 8.7$ Hz, 2 H), 8.37 (s, 1 H), 8.24 (d, $J = 8.7$ Hz, 2 H), 8.11 (d, $J = 3.7$ Hz, 1 H), 8.04 (dt, $J = 1.6$, 7.6 Hz, 2 H), 7.73 (d, $J = 5.0$ Hz, 2 H), 7.53 (dd, $J = 4.9$, 7.4 Hz, 1 H), 7.25 (dd, $J = 4.8$, 3.9 Hz, 1 H) ppm. ^{13}C NMR ($[\text{D}_6]\text{dmsO}$, 75 MHz): $\delta = 156.5$, 155.2, 153.4, 150.2, 148.8, 148.0, 144.9, 144.4, 138.4, 130.0, 129.43, 129.41, 127.4, 125.6, 125.1, 121.6, 117.6, 117.2 ppm.

4-(4-tert-Butylphenyl)-6-(5-methylthiophen-2-yl)-2,2'-bipyridine (L6): Yellow crystals (39%). M.p. 162.0–164.8 °C. FT-IR: $\tilde{\nu} = 2963.2$ (m), 2866.5 (w), 1596.0 (s), 1581.9 (s), 1566.0 (s), 1539.5 (s), 1479.6 (s), 1389.2 (s), 1244.7 (w), 1116.8 (w), 1017.0 (w), 830.7 (s), 794.2 (s), 743.66 (w), 541.9 (w) cm^{-1} . ^1H NMR (CDCl_3 , 300 MHz): $\delta = 8.70$ (d, $J = 4.2$ Hz, 1 H), 8.61 (d, $J = 8.0$ Hz, 1 H), 8.52 (d, $J = 1.4$ Hz, 1 H), 7.86 (td, $J = 7.6$, 1.8 Hz, 1 H), 7.81 (d, $J = 1.5$ Hz, 1 H), 7.75 (d, $J = 8.5$ Hz, 2 H), 7.54 (d, $J = 8.6$ Hz, 2 H), 7.54 (d, $J = 2.0$ Hz, 1 H), 7.33 (dd, $J = 4.8$, 1.2 Hz, 1 H), 6.81 (dd, $J = 3.6$, 0.9 Hz, 1 H), 2.58 (s, 3 H), 1.45 (s, 9 H) ppm. ^{13}C NMR (CDCl_3 , 75 MHz): $\delta = 160.2$, 159.9, 156.3, 156.2, 153.9, 153.0, 147.0, 146.4, 140.9, 139.6, 130.9, 130.3, 129.9, 128.6, 127.7, 125.5, 120.7, 120.0, 38.7, 35.3 ppm.

4-(4-Methoxyphenyl)-6-(5-methylthiophen-2-yl)-2,2'-bipyridine (L7): Yellow crystals (20%). M.p. 150.0–155.0 °C. FT-IR: $\tilde{\nu} = 3435.0$ (w), 2914.0 (w), 1608.4 (s), 1598.2 (s), 1517 (s), 1423.4 (s), 1254.7 (s), 1184.8 (s), 1110.8 (m), 1029.6 (s), 837.1 (m), 797.0 (s), 744.6 (m), 574.0 (m) cm^{-1} . ^1H NMR (CDCl_3 , 300 MHz): $\delta = 8.69$ (d, $J = 0.9$ Hz, 1 H), 8.60 (d, $J = 7.8$ Hz, 1 H), 8.48 (d, $J = 1.5$ Hz, 1 H), 7.85 (td, $J = 7.5$, 1.8 Hz, 1 H), 7.78 (s, 1 H), 7.77 (d, $J = 9.0$ Hz, 2 H), 7.46 (d, $J = 3.6$ Hz, 1 H), 7.36 (dd, $J = 5.6$, 1.2 Hz, 1 H), 7.04 (d, $J = 9.0$ Hz, 2 H), 6.82 (dd, $J = 3.6$, 1.2 Hz, 1 H), 3.89 (s, 3 H), 2.55 (s, 3 H) ppm. ^{13}C NMR (CDCl_3 , 75 MHz): $\delta = 160.8$, 156.1, 156.1, 156.7, 149.8, 149.2, 143.1, 142.6, 137.1, 131.1, 128.6, 126.5, 124.8, 124.0, 121.7, 116.5, 115.8, 114.6, 55.4, 16.2 ppm.

6-(5-Methylthiophen-2-yl)-4-(4-nitrophenyl)-2,2'-bipyridine (L8): Yellow needles (3.5%). M.p. 212.8–214.1 °C. FT-IR: $\tilde{\nu} = 3413.5$ (w), 3052.1 (w), 2917.4 (w), 2850.0 (w), 1595.1 (m), 1566.9 (m), 1584.6 (s), 1471.0 (s), 1345.0 (s), 1248.1 (m), 1108.3 (m), 852.1 (m), 754.8 (m), 741.4 (w), 696.28 (w), 616.3 (w), 469.5 (w) cm^{-1} . ^1H NMR ($[\text{D}_6]\text{dmsO}$, 300 MHz): $\delta = 8.70$ (d, $J = 4.7$ Hz, 1 H), 8.62

(d, $J = 8.0$ Hz, 1 H), 8.52 (d, $J = 1.4$ Hz, 1 H), 8.37 (d, $J = 8.8$ Hz, 2 H), 7.94 (d, $J = 8.8$ Hz, 2 H), 7.89 (td, $J = 7.7$, 1.7 Hz, 1 H), 7.78 (d, $J = 1.4$ Hz, 1 H), 7.55 (d, $J = 3.6$ Hz, 1 H), 7.36 (dd, $J = 4.8$, 1.1 Hz, 1 H), 6.81 (d, $J = 3.6$, 1.2 Hz, 1 H), 2.58 (s, 3 H) ppm. ^{13}C NMR ($[\text{D}_6]\text{dmsO}$, 75 MHz): $\delta = 156.8$, 156.0, 153.4, 149.5, 148.6, 148.1, 145.5, 143.6, 142.6, 137.5, 128.6, 126.9, 125.6, 124.7, 124.6, 122.0, 117.1, 116.5, 16.1 ppm.

6-(5-Methylthiophen-2-yl)-4-(thiophen-2-yl)-2,2'-bipyridine (L9): Yellow crystals (47%). M.p. 116.8–121.0 °C. FT-IR: $\tilde{\nu} = 2909.4$ (w), 1596.3 (m), 1581.9 (m), 1556.6 (m), 1543.0 (m), 1403.5 (m), 789.0 (s), 694.3 (s) cm^{-1} . ^1H NMR (CDCl_3 , 300 MHz): $\delta = 8.71$ (d, $J = 4.8$ Hz, 1 H), 8.58 (d, $J = 8.1$ Hz, 1 H), 8.49 (d, $J = 1.5$ Hz, 1 H), 7.86 (td, $J = 7.5$, 1.8 Hz, 1 H), 7.77 (d, $J = 1.5$ Hz, 1 H), 7.68 (dd, $J = 3.6$, 1.8 Hz, 1 H), 7.53 (d, $J = 3.60$ Hz, 1 H), 7.44 (dd, $J = 5.1$, 1.2 Hz, 1 H), 7.34 (dd, $J = 4.8$, 1.2 Hz, 1 H), 7.17 (dd, $J = 5.1$, 3.6 Hz, 1 H), 6.82 (dd, $J = 3.6$, 1.2 Hz, 1 H), 2.58 (s, 3 H) ppm. ^{13}C NMR (CDCl_3 , 75 MHz): $\delta = 156.5$, 156.2, 153.1, 149.4, 143.4, 143.1, 142.9, 142.1, 137.3, 128.7, 127.4, 126.8, 126.0, 125.2, 124.3, 121.9, 115.4, 114.8, 16.2 ppm.

L10, L11 and L12 were prepared as reported earlier.^[8] Experimental schemes are enclosed in the Supporting Information.

L13 was prepared via the intermediate compounds **14–16**.

3-[2-(Pyridin-2-yl)vinyl]-2-1,3-dioxolan-2-yl]thiophene (14): 2-(3-Bromothiophen-2-yl)-1,3-dioxolane^[9] (1.65 g, 7 mmol), 2-vinylpyridine (0.75 g, 7 mmol) and potassium carbonate (1.93 g, 14 mmol) were dissolved in DMF (20 mL, dried with molecular sieves). The solution was thoroughly stirred for 10 min before the addition of tetrakis(triphenylphosphane)palladium (40 mg, 35 μmol , 0.5 mol-%). The solution was refluxed, and the reaction was monitored by TLC. After 8 h, TLC indicated that all starting material had been consumed, and the reaction mixture was poured into water (200 mL). The resulting precipitate was filtered through a fine sintered glass funnel and became a viscous oil on the funnel surface. Extraction with boiling heptane provided **14**, which was further purified by flash chromatography [silica, hexane/EtOAc (1:1)]. Product appearance: viscous yellow oil. Yield: 1.71 g (94%). ^1H NMR (300 MHz, CDCl_3): $\delta = 8.60$ (d, $J = 4.8$ Hz, 1 H), 7.76 (d, $J = 16.0$ Hz, 1 H), 7.65 (dt, $J = 1.8$, 7.7 Hz, 1 H), 7.37 (d, $J = 8.0$ Hz, 1 H), 7.35 (d, $J = 5.3$ Hz, 1 H), 7.28 (d, $J = 5.3$ Hz, 1 H), 7.14 (ddd, $J = 1.1$, 4.8, 7.5 Hz, 1 H), 7.04 (d, $J = 16.0$ Hz, 1 H), 6.37 (s, 1 H), 4.23–4.00 (m, 4 H) ppm. ^{13}C NMR (CDCl_3 , 75 MHz): $\delta = 155.7$, 149.8, 138.6, 137.5, 136.7, 129.7, 126.0, 125.8, 124.4, 122.3, 122.2, 99.1, 65.6 ppm. MS: $m/z = 259$ [M^+]. $\text{C}_{14}\text{H}_{13}\text{NO}_2\text{S}$ (259.32): calcd. C 64.84, H 5.05, N 5.40; found C 64.68, H 4.88, N 5.29.

3-[2-(Pyridin-2-yl)vinyl]thiophene-2-carbaldehyde (15): A solution of KHSO_4 (0.90 g, 6.6 mmol) in H_2O (5 mL) was added to a solution of **14** (1.55 g, 6.0 mmol) in acetone (20 mL). The mixture instantly turned cloudy and yellow. The mixture was refluxed, and, after 2 h, TLC showed the total consumption of the starting material. The acetone was evaporated, and water was added (200 mL), thus dissolving most of the inorganic precipitate. The solution was extracted with dichloromethane (3×50 mL), the organic extracts were combined and were dried with anhydrous MgSO_4 and concentrated to provide pure **15**. Product appearance: viscous yellow oil. Yield: 1.12 g (87%). ^1H NMR (300 MHz, CDCl_3): $\delta = 10.31$ (s, 1 H), 8.64 (d, $J = 4.6$ Hz, 1 H), 8.20 (d, $J = 15.9$ Hz, 1 H), 7.75–7.67 (m, 2 H), 7.49 (d, $J = 5.1$ Hz, 1 H), 7.43 (d, $J = 7.8$ Hz), 7.26–7.18 (m, 2 H) ppm. MS: $m/z = 215$ [M^+]. $\text{C}_{12}\text{H}_9\text{NOS}$ (215.27): calcd. C 66.95, H 4.21, N 6.51; found C 67.07, H 4.37, N 6.40.

3-[2-(Pyridin-2-yl)vinyl]thiophene-2-carbaldehyde Oxime (16): The aldehyde **15** (1.04 g, 4.8 mmol), hydroxylamine hydrochloride

(0.67 g, 9.7 mmol) and sodium acetate (0.79 g, 9.7 mmol) were added to ethanol (16 mL), and the mixture was refluxed. The reaction was monitored by TLC and stopped when no starting material was present anymore. Two products [(*E*) and (*Z*) isomers] were detected. The ethanol was evaporated, and H₂O (50 mL) was added to the oily residue. The mixture was then extracted with dichloromethane (3 × 50 mL) and then with ethyl acetate (3 × 50 mL). The isomers show different solubility characteristics in the two solvents, although this was not investigated further. The organic extracts were combined, dried with anhydrous MgSO₄ and concentrated to afford **16** sufficiently pure for the following step. Product appearance: yellow powder. Yield: 1.09 g (99%). ¹H NMR (300 MHz, CDCl₃): (*E*) isomer: δ = 8.73 (s, 1 H), 8.64 (d, *J* = 4.8 Hz, 1 H), 7.89 (d, *J* = 15.8 Hz, 1 H), 7.70 (dt, *J* = 2.0, 7.7 Hz, 1 H), 7.39 (d, *J* = 7.8 Hz, 1 H), 7.36 (d, *J* = 5.5 Hz, 1 H), 7.29 (d, *J* = 5.4 Hz, 1 H), 7.20 (m, 1 H), 7.05 (d, *J* = 15.8 Hz, 1 H) ppm; (*Z*) isomer: δ = 8.64 (d, *J* = 4.8 Hz, 1 H), 8.17 (s, 1 H), 7.97 (d, *J* = 15.8 Hz, 1 H), 7.71 (dt, *J* = 2.0, 7.7 Hz, 1 H), 7.53 (d, *J* = 5.4 Hz, 1 H), 7.43 (d, *J* = 5.3 Hz, 1 H), 7.39 (d, *J* = 7.8 Hz, 1 H), 7.20 (m, 1 H), 7.12 (d, *J* = 15.8 Hz, 1 H) ppm. MS: *m/z* = 230 [M⁺]. C₁₂H₁₀N₂OS (230.28): calcd. C 62.59, H 4.38, N 12.16; found C 62.71, H 4.52, N 12.01.

5-(Pyridin-2-yl)thieno[2,3-*c*]pyridine (L13): The oxime **16** (1.05 g, 4.95 mmol) was dissolved in decahydronaphthalene (50 mL) and refluxed. The reaction was monitored by TLC, and, when no starting material was left anymore, the reaction was stopped. The solvent was removed by vacuum distillation, and the remaining black oil was dissolved in dichloromethane (50 mL), which was extracted with dilute hydrochloric acid (3 × 50 mL). The aqueous phase was made alkaline with Na₂CO₃ and then extracted with dichloromethane (3 × 50 mL), dried with anhydrous MgSO₄ and concentrated to yield a viscous black oil which solidified upon standing. The black solid was triturated with boiling heptane, which, after evaporation, yielded a yellow low-melting solid. Recrystallization from methanol afforded pure **L13**. Product appearance: off-white prisms. Yield: 0.37 g (35%). M.p. 122–124 °C. ¹H NMR (300 MHz, CDCl₃): δ = 9.21 (s, 1 H), 8.83 (d, *J* = 0.9 Hz, 1 H), 8.70 (ddd, *J* = 7.8, 1.7, 0.8 Hz, 1 H), 8.47 (dt, *J* = 8.0, 0.9 Hz, 1 H), 7.83 (dt, *J* = 7.7, 1.8 Hz, 1 H), 7.72 (d, *J* = 5.4 Hz, 1 H), 7.46 (dd, *J* = 5.4, 0.6 Hz, 1 H), 7.30 (ddd, *J* = 7.5, 4.8, 1.2 Hz, 1 H) ppm. ¹³C NMR (CDCl₃, 75 MHz): δ = 156.6, 150.6, 149.4, 146.2, 144.1, 137.2, 136.7, 132.6, 124.0, 123.5, 121.4, 115.4 ppm. MS: *m/z* = 212 [M⁺]. C₁₂H₈N₂S (212.27): calcd. C 67.90, H 3.80, N 13.20; found C 67.78, H 3.86, N 13.11.

Representative Procedure for the Preparation of the Propenones P2–P9

3-(4-*tert*-Butylphenyl)-1-(2-thiophen-2-yl)propenone (P3): NaOH (2.5 g, 62.5 mmol) was dissolved in a mixture of ethanol (30 mL) and water (20 mL) and well cooled with ice. 4-*tert*-Butylbenzaldehyde (4.87 g, 30 mmol) was added in 5 portions over 5 min, and then 2-acetylthiophene (3.80 g, 30 mmol) was added dropwise over 20 min to the reaction mixture. The mixture was protected from light and stirred vigorously for 48 h, during which time the temperature was allowed to rise to room temperature. The product was extracted with dichloromethane (3 × 50 mL), and the collected organic phases were dried with MgSO₄ before the solvent was evaporated. The residue was recrystallized from methanol to give the pure product. Product appearance: yellow crystals. Yield: 5.84 g (72%). M.p. 79.3–80.0 °C. FT-IR: $\tilde{\nu}$ = 3087 (m), 2961 (s), 1644 (s), 1583 (s), 1558 (m), 1516 (m), 1456 (w), 1417 (s), 1354 (s) cm⁻¹. ¹H NMR (CDCl₃, 300 MHz): δ = 7.87 (dd, *J* = 1.2, 3.9 Hz, 1 H), 7.85 (d, *J* = 15.5 Hz, 1 H), 7.68 (dd, *J* = 1.1, 5.0 Hz, 1 H), 7.60 (d, *J* = 8.4 Hz, 2 H), 7.45 (d, *J* = 8.4 Hz, 2 H), 7.39 (d, *J* = 15.6 Hz, 1 H),

7.19 (dd, *J* = 3.8, 4.9 Hz, 1 H), 1.35 (s, 9 H) ppm. ¹³C NMR (CDCl₃, 75 MHz): δ = 182.6, 154.7, 146.1, 144.45, 134.2, 132.4, 132.2, 128.8, 128.7, 126.4, 121.2, 35.4, 31.8 ppm.

3-(Thiophen-2-yl)propenal (P2): Pale yellow oil (61%). FT-IR: $\tilde{\nu}$ = 2424.8 (w), 1665.1 (s), 1608.5 (s), 1421.0 (m), 1225.8 (w), 1113.3 (m), 1044.2 (w), 958.5 (m), 856.4 (m), 702.6 (s) cm⁻¹. ¹H NMR (CDCl₃, 300 MHz): δ = 9.60 (d, *J* = 7.7 Hz, 1 H), 7.58 (d, *J* = 15.6 Hz, 1 H), 7.49 (d, *J* = 5.1 Hz, 1 H), 7.36 (d, *J* = 3.1 Hz, 1 H), 7.10 (dd, *J* = 5.1, 3.7 Hz, 1 H), 6.49 (dd, *J* = 15.6, 7.7 Hz, 1 H) ppm. ¹³C NMR (CDCl₃, 75 MHz): δ = 193.0, 144.6, 139.3, 132.3, 130.5, 128.6, 127.3 ppm.

3-(4-Methoxyphenyl)-1-(thiophen-2-yl)propenone (P4): Yellow crystals (76%). M.p. 84.5–86.0 °C (ref.^[18] 87 °C). FT-IR: $\tilde{\nu}$ = 1647 (s), 1595 (s), 1512 (s), 1459 (w), 1413 (m), 1355 (w), 1299 (w), 1268 (m), 1229 (m), 1219 (m), 1174 (m), 1065 (w), 1016 (m), 981 (m), 855 (w), 819 (s), 741 (m), 514 (w) cm⁻¹. ¹H NMR (CDCl₃, 300 MHz): δ = 7.86 (dd, *J* = 1.2, 3.7 Hz, 1 H), 7.83 (d, *J* = 15.5 Hz, 1 H), 7.66 (dd, *J* = 1.1, 4.9 Hz, 1 H), 7.61 (d, *J* = 8.7 Hz, 2 H), 7.31 (d, *J* = 15.5 Hz, 1 H), 7.18 (dd, *J* = 3.8, 4.9 Hz, 1 H), 6.94 (d, *J* = 8.8 Hz, 2 H), 3.88 (s, 3 H) ppm. ¹³C NMR (CDCl₃, 75 MHz): δ = 182.5, 162.1, 146.2, 144.3, 134.0, 132.0, 130.7, 128.6, 127.8, 119.6, 114.8, 55.8 ppm.

3-(4-Nitrophenyl)-1-(thiophen-2-yl)propenone (P5): Yellow powder (69%). M.p. 225.0–226.0 °C (ref.^[19] 220 °C). FT-IR: $\tilde{\nu}$ = 1951 (s), 1605 (m), 1513 (s), 1411 (m), 1338 (s), 1290 (w), 1240 (w), 1223 (w), 1107 (w), 1086 (w), 975 (w), 862 (w), 841 (w), 762 (w), 741 (m) cm⁻¹. ¹H NMR ([D₆]dmsO, 300 MHz): δ = 8.41 (dd, *J* = 4.2, 0.5 Hz, 1 H), 8.29 (d, *J* = 8.8 Hz, 2 H), 8.17 (d, *J* = 8.86 Hz, 2 H), 8.12 (dd, *J* = 0.5, 4.4 Hz, 1 H), 8.08 (d, *J* = 15.6 Hz, 1 H), 7.82 (d, *J* = 15.6 Hz, 1 H), 7.33 (dd, *J* = 4.3, 4.5 Hz, 1 H) ppm. ¹³C NMR ([D₆]dmsO, 75 MHz): δ = 182.2, 149.0, 146.0, 141.9, 141.2, 137.3, 135.4, 130.8, 130.0, 126.7, 124.8 ppm.

3-(4-*tert*-Butylphenyl)-1-(5-methylthiophen-2-yl)propenone (P6): Yellow needles (69%). M.p. 89.1–89.8 °C. FT-IR: $\tilde{\nu}$ = 3070.8 (w), 3052.9 (w), 2960.1 (s), 1647.7 (s), 1599.2 (s), 1514.0 (m), 1458.3 (s), 1385.1 (w), 1365.1 (m), 1333.2 (m), 1244.1 (m), 1222.3 (m), 1073.8 (m), 980.2 (s), 812.8 (s), 555.0 (m) cm⁻¹. ¹H NMR (CDCl₃, 300 MHz): δ = 7.81 (d, *J* = 15.6 Hz, 1 H), 7.69 (d, *J* = 3.8 Hz, 1 H), 7.58 (d, *J* = 8.4 Hz, 2 H), 7.44 (d, *J* = 8.4 Hz, 2 H), 7.5 (d, *J* = 15.6 Hz, 1 H), 6.85 Hz (dd, *J* = 3.8, 0.95 Hz, 1 H), 2.57 (d, *J* = 0.95 Hz, 3 H), 1.34 (s, 9 H) ppm. ¹³C NMR (CDCl₃, 75 MHz): δ = 181.9, 154.2, 150.1, 143.7, 143.5, 132.5, 132.3, 128.5, 127.1, 126.1, 120.9, 35.1, 31.3, 16.3 ppm.

3-(4-Methoxyphenyl)-1-(5-methylthiophen-2-yl)propenone (P7): Yellow crystals (92%). M.p. 118.0–119.5 °C. FT-IR: $\tilde{\nu}$ = 1639.9 (s), 1570.2 (s), 1513.5 (m), 1453.7 (m), 1310.7 (w), 1297.4 (m), 1261.2 (w), 1238.5 (m), 1223.4 (m), 1176.6 (s), 1071.1 (m), 1029.8 (w), 986.1 (m), 830.9 (w), 802.0 (s), 719.6 (w) cm⁻¹. ¹H NMR (CDCl₃, 300 MHz): δ = 7.79 (d, *J* = 15.5 Hz, 1 H), 7.67 (d, *J* = 3.6 Hz, 1 H), 7.59 (d, *J* = 8.7 Hz, 2 H), 7.26 (d, *J* = 15.5 Hz, 1 H), 6.94 (d, *J* = 8.7 Hz, 2 H), 6.85 (dd, *J* = 2.8, 1.0 Hz, 1 H), 3.85 (s, 3 H), 2.59 (s, 3 H) ppm. ¹³C NMR (CDCl₃, 75 MHz): δ = 181.9, 161.8, 149.9, 143.4, 132.3, 130.4, 127.8, 127.1, 119.4, 114.6, 55.6, 16.3 ppm.

1-(5-Methylthiophen-2-yl)-3-(4-nitrophenyl)propenone (P8): Orange powder (92%). M.p. 191.6–197.1 °C. FT-IR: $\tilde{\nu}$ = 2155.9 (w), 1643.9 (m), 1588.0 (m), 1509.4 (m), 1455.5 (m), 1336.8 (s), 1236.6 (m), 985.0 (m), 806.3 (s), 667.7 (s) cm⁻¹. ¹H NMR ([D₆]dmsO, 300 MHz): δ = 8.30 (d, *J* = 8.7 Hz, 2 H), 8.23 (d, *J* = 3.9 Hz, 1 H), 8.14 (d, *J* = 8.7 Hz, 2 H), 8.03 (d, *J* = 15.7 Hz, 1 H), 7.77 (d, *J* = 15.7 Hz, 1 H), 7.05 (d, *J* = 3.0 Hz, 1 H), 2.55 (s, 3 H) ppm. ¹³C NMR ([D₆]dmsO, 75 MHz): δ = 180.9, 148.1, 143.2, 141.2, 140.0, 135.3, 134.7, 129.9, 128.0, 127.3, 124.0, 16.0 ppm.

1-(5-Methylthiophen-2-yl)-3-(thiophen-2-yl)propenone (P9): Yellow crystals (71%). M.p. 108.3–110.0 °C. FT-IR: $\tilde{\nu}$ = 1637.2 (m), 1577.8 (m), 1454.4 (m), 1277.7 (m), 1212.8 (m), 1065.0 (m), 1039.7 (m), 957.2 (s), 863.6 (m), 827.2 (m), 796.0 (s), 714.0 (s) cm^{-1} . ^1H NMR (CDCl_3 , 300 MHz): δ = 7.93 (d, J = 15.3 Hz, 1 H), 7.66 (d, J = 3.9 Hz, 1 H), 7.41 (d, J = 5.1 Hz, 1 H), 7.34 (d, J = 3.3 Hz, 1 H), 7.17 (d, J = 15.3 Hz, 1 H), 7.09 (dd, J = 5.1, 3.6 Hz, 1 H), 6.85 (d, J = 4.5 Hz, 1 H), 2.55 (s, 3 H) ppm. ^{13}C NMR (CDCl_3 , 75 MHz): δ = 181.6, 150.6, 143.8, 140.7, 136.2, 132.8, 132.4, 129.0, 128.7, 127.4, 120.7, 16.6 ppm.

Supporting Information (see footnote on the first page of this article): Reaction schemes for ligands **L10–L12**. Cyclic voltammograms for complex **C1–C13**. ^1H NMR spectra of ligands **L1–L13**. ^1H NMR and COSY spectra of complexes **C1–C13**. UV/Vis spectra of complexes **C1–C13**.

Acknowledgments

The authors would like to thank Fakultetsnämnden (Naturvetenskap och teknik), Mälardalen University, for their generous and continued support of this project. R. O. S. would like to thank the Dentist Gustav Dahl Memorial Fund for generous support. The authors also would like to thank Mr. George Blazak at the University of Queensland, Australia, for performing elemental analysis and Dr. Conor Brennan at the University of Basel, Switzerland, for performing MALDI-TOF analysis.

- [1] P. Bäuerle in *Electronic Materials: The Oligomer Approach* (Eds.: K. Müllen, G. Wegner), Wiley-VCH, Weinheim, **1998**, p. 105.
- [2] *Handbook of Oligo- and Polythiophenes* (Ed.: D. Fichou), Wiley-VCH, Weinheim, **1999**, and references therein.
- [3] a) S. Campagna, F. Puntoriero, F. Nastasi, G. Bergamini, V. Balzani, *Top. Curr. Chem.* **2007**, 280, 117–214; b) K. Kalyanasundaram, *Photochemistry of Polypyridine and Porphyrin Complexes*, Academic Press Ltd., London, **1992**.

- [4] A. C. Benniston, A. Harriman, *Chem. Soc. Rev.* **2006**, 35, 169–179.
- [5] R. O. Steen, L. J. Nurkkala, S. J. Angus-Dunne, C. X. Schmitt, E. C. Constable, M. J. Riley, P. V. Bernhardt, S. J. Dunne, *Eur. J. Inorg. Chem.* **2008**, 1784–1794.
- [6] F. Kröhnke, *Synthesis* **1976**, 1, 1–24.
- [7] E. C. Constable, R. P. G. Henney, T. A. Leese, *J. Organomet. Chem.* **1989**, 361, 277–282.
- [8] L. J. Nurkkala, R. O. Steen, S. J. Dunne, *Synthesis* **2006**, 8, 1295–1300.
- [9] J. D. Prugh, G. D. Hartman, P. J. Mallorga, B. M. McKeever, S. R. Michelson, M. A. Murcko, H. Schwam, R. L. Smith, J. M. Sondey, J. P. Springer, M. F. Sugrue, *J. Med. Chem.* **1991**, 34, 1805–1818.
- [10] S. Hibino, S. Kano, N. Mochizuki, E. J. Sugino, *J. Org. Chem.* **1984**, 49, 5006.
- [11] R. F. Jones, D. J. Cole-Hamilton, *Inorg. Chim. Acta* **1981**, 53, L3.
- [12] B. Durham, J. L. Walsh, C. L. Carter, T. J. Meyer, *Inorg. Chem.* **1980**, 19, 860–865.
- [13] a) W. K. Seok, T. J. Meyer, *Inorg. Chem.* **2005**, 44, 3931–3941; b) G. M. Brown, R. W. Callahan, T. J. Meyer, *Inorg. Chem.* **1975**, 14, 1915–1921; c) F. Xu, W. Huang, *Acta Crystallogr., Sect. E* **2007**, 63, m2114.
- [14] A. Juris, V. Balzani, F. Barigelletti, S. Campagna, P. Belser, A. Von Zelevsky, *Coord. Chem. Rev.* **1988**, 84, 85–277.
- [15] J. Van Houten, R. J. Watts, *J. Am. Chem. Soc.* **1976**, 98, 4853–4858.
- [16] J. P. Sauvage, J. P. Collin, J. C. Chambron, S. Guillerez, C. Coudret, V. Balzani, F. Barigelletti, L. De Cola, L. Flamigni, *Chem. Rev.* **1994**, 94, 993–1019.
- [17] J. N. Demas, G. A. Crosby, *J. Phys. Chem.* **1971**, 75, 991–1024.
- [18] L. Greiner-Bechert, H.-H. Otto, *Arch. Pharm. (Weinheim Ger.)* **1991**, 324, 563–572.
- [19] N. P. Buu-Hoi, N. D. Xuong, M. Sy, *Bull. Soc. Chim. Fr.* **1956**, 1646–1650.

Received: May 6, 2008

Published Online: August 4, 2008